

## Article

# Study on the Adaptability Evaluation of Micro-Dispersed-Gel-Strengthened-Alkali-Compound System and the Production Mechanism of Crude Oil

Teng Wang <sup>1</sup>, Tianjiang Wu <sup>1,\*</sup>, Yunlong Liu <sup>1</sup>, Chen Cheng <sup>1</sup> and Guang Zhao <sup>2</sup>

<sup>1</sup> Oil and Gas Technology Research Institute, PetroChina Changqing Oilfield Company, Xi'an 710016, China; wangteng0822@163.com (T.W.); liuyunl\_cq@petrochina.com.cn (Y.L.); chchen\_cq@petrochina.com.cn (C.C.)

<sup>2</sup> School of Petroleum Engineering, China University of Petroleum (East China), Qingdao 266580, China; zhaoguang@upc.edu.cn

\* Correspondence: 579520@163.com; Tel.: +86-029-86590702

**Abstract:** A novel micro-dispersed-gel (MDG)-strengthened-alkali-compound flooding system was proposed for enhanced oil recovery in high-water-cut mature oilfields. Micro-dispersed gel has different adaptability and application schemes with sodium carbonate and sodium hydroxide. The MDG-strengthened-alkali flooding system can reduce the interfacial tension to an ultra-low interfacial-tension level of  $10^{-2}$  mN/m, which can reverse the wettability of rock surface. After 30 days aging, the MDG-strengthened- $\text{Na}_2\text{CO}_3$  flooding system has good viscosity retention of 74.5%, with an emulsion stability of 79.13%. The enhanced-oil-recovery ability of the MDG-strengthened- $\text{Na}_2\text{CO}_3$  (MDGSC) flooding system is 43.91%, which is slightly weaker than the 47.78% of the MDG-strengthened- $\text{NaOH}$  (MDGSH) flooding system. The crude-oil-production mechanism of the two systems is different, but they all show excellent performance in enhanced oil recovery. The MDGSC flooding system mainly regulates and seals micro-fractures, forcing subsequent injected water to enter the low-permeability area, and it has the ability to wash the remaining oil in micro-fractures. The MDGSH flooding system mainly removes the remaining oil on the rock wall surface in the micro-fractures by efficient washing, and the MDG particles can also form weak plugging of the micro-fractures. The MDG-strengthened-alkali flooding system can be used as an alternative to enhance oil recovery in high-water-cut and highly heterogeneous mature oilfields.

**Keywords:** MDG-strengthened-alkali-compound system; adaptability evaluation; low interfacial tension (IFT); strong wetting change ability; oil-production mechanism



**Citation:** Wang, T.; Wu, T.; Liu, Y.; Cheng, C.; Zhao, G. Study on the Adaptability Evaluation of Micro-Dispersed-Gel-Strengthened-Alkali-Compound System and the Production Mechanism of Crude Oil. *Processes* **2024**, *12*, 871. <https://doi.org/10.3390/pr12050871>

Academic Editor: Albert Ratner

Received: 28 March 2024

Revised: 13 April 2024

Accepted: 17 April 2024

Published: 26 April 2024



**Copyright:** © 2024 by the authors. Licensee MDPI, Basel, Switzerland. This article is an open access article distributed under the terms and conditions of the Creative Commons Attribution (CC BY) license (<https://creativecommons.org/licenses/by/4.0/>).

## 1. Introduction

Since the development of the old oilfield bringing the 'double high' stage of high water cut and high oil-recovery degree [1–3], it is more and more difficult to stabilize the production of water flooding, and the oilfield development situation is grim. In the process of water flooding, it is more and more difficult to improve oil recovery, and the water cut of oil wells is also increasing. In the late stage of oilfield development, long-term water injection will affect the pore medium in the reservoir, resulting in reservoir heterogeneity [4–6], thus greatly reducing water-injection efficiency and oil recovery [7,8]. In order to change the current situation of high water cut in oil wells and improve oil recovery, reasonable measures must be taken to control the high permeability channels between oil and water wells [9,10]. The chemical flooding method [11–14] is widely used in oilfields to improve oil recovery because it can improve water–oil mobility [15,16] and reduce oil–water interfacial tension [15,17,18]. It is an effective and widely used method to solve the problem of high water cut and low recovery. It has become an important technology to greatly improve crude oil recovery.

The chemical flooding [19] method mainly includes polymer flooding, surfactant flooding, alkali flooding, compound flooding, and heterogeneous-compound flooding [20,21] proposed in recent years. In the process of polymer flooding, the mechanism of mobility control, change of water absorption profile, and expansion of swept volume [22,23] can be seen. In the process of surfactant flooding [24,25] or alkali flooding [26,27], the mechanism of low interfacial tension, wettability change, and emulsified oil can be seen. At present, chemical methods can be used to improve oil recovery and expand the swept volume and improve oil-displacement efficiency. Although polymer flooding or polymer/alkali flooding technology [28,29] has been successfully applied to oil fields to improve oil recovery, there are still inherent shortcomings. The polymer is easy to be sheared by mechanical equipment, and the formation temperature or alkali addition in compound flooding led to hydrolysis, resulting in loss of viscosity of polymer solution and weakening of mobility control [30,31]. At present, the heterogeneous-compound flooding based on micro-dispersed gel can expand the sweep by the viscosity of the micro-dispersed-gel solution plugging the water channel [32–34]. By combining the micro-dispersed gel [35] with the surfactant, the mechanism of plugging the high-permeability channel [36,37], low interfacial tension [38–41], and wettability reversal [42,43] can be realized in the displacement stage to improve the oil recovery rate.

In order to further improve the oil recovery in the late stage of oilfield development, this paper proposes a heterogeneous-compound oil-displacement system based on micro-dispersed gel, which is composed of micro-dispersed gel and alkali. The adaptability and basic physical and chemical properties are evaluated, and the crude-oil-production mechanism of the micro-dispersed-gel-strengthened-alkali-compound system is clarified. The micro-dispersed gel has good viscoelasticity, which can play a role in profile control, expand the swept volume, and solve the problem of fingering in alkali flooding. Alkali can react with crude oil to form oil soap in situ to achieve ultra-low interfacial tension, change the oil–water interface properties, and improve oil-displacement efficiency. The two work together efficiently to achieve the purpose of improving crude oil recovery. By evaluating the basic properties of the compound system and core flow experiments, the adaptability and basic properties of the micro-dispersed-gel-strengthened-alkali-compound flooding system were clarified, and its enhanced-oil-recovery ability and crude-oil-production mechanism were discussed, which provided a basis for the establishment of a new method for enhanced oil recovery.

## 2. Experimental Procedures

### 2.1. Materials

Hydrophobically associating polymer (HAP) with a hydrolysis degree of 20% and an average molecular weight of 14,000,000 was obtained from Gaoyuan Co., Ltd. (Dongying, China). Analytically pure sodium carbonate was obtained from Guoyao Co., Ltd. (Shanghai, China) Analytically pure sodium hydroxide was obtained from Guoyao Co., Ltd. (Shanghai, China). The viscosity of the simulated oil was 15 mPa·s at 50 °C, which was provided by the Changqing oilfield in China. The salinity of the simulated water used in the following experiments was 49,350 mg/L (NaCl: 29,328 mg/L, CaCl<sub>2</sub>: 1768 mg/L, MgCl<sub>2</sub>: 387 mg/L).

### 2.2. Preparation Method of MDG

MDG is prepared by mechanical shearing. The preparation method is divided into two stages: bulk-gel crosslinking stage and MDG mechanical-shearing stage. First, a polymer solution with a mass concentration of 0.3% was prepared using simulated water, and then, the cross-linking agent was slowly added to the polymer solution and stirred evenly at room temperature to form a glue solution. Then, the gelling solution was sealed and placed in a 90 °C oven for 72 h of crosslinking reaction to form a bulk gel. Secondly, the bulk gel was placed in a colloid mill for mechanical shearing and grinding for 10 min to obtain an MDG solution. Figure 1 shows the micromorphology and average size of the MDG.

The size of the MDG was measured by dynamic light scattering (DLS, Bruker-Nano, Bruker Instruments Ltd., Berlin, Germany) and scanning electron microscopy (SEM, Hitachi S-4800, Hitachi High-Technologies Co., Ltd., Tokyo, Japan), and the initial average size of the MDG was 505 nm.

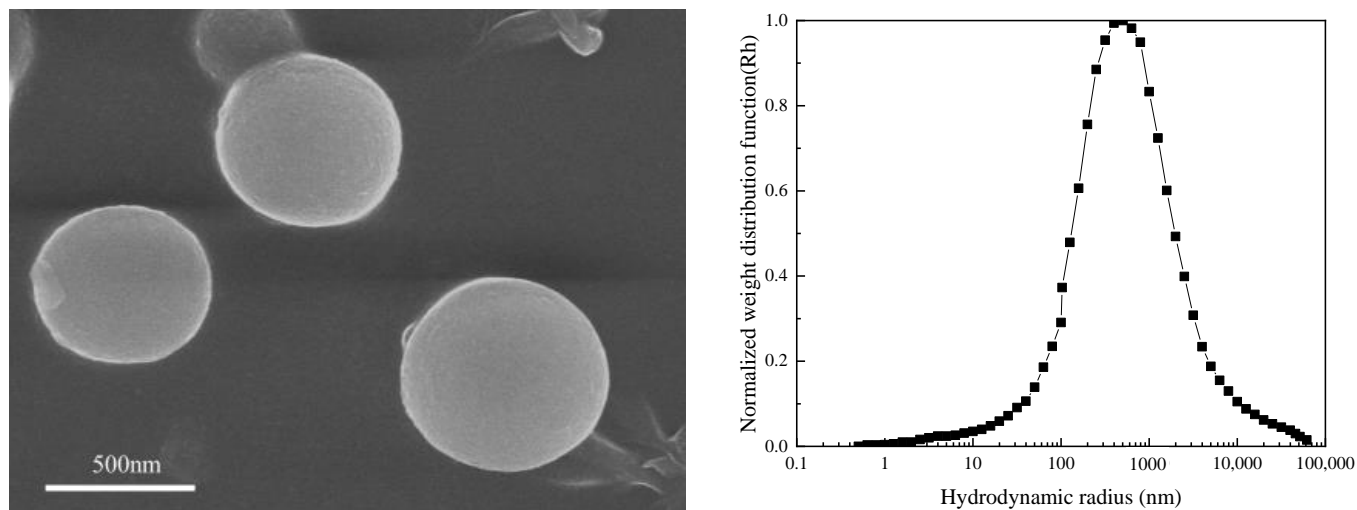


**Figure 1.** The micromorphology and average size of the MDG.

### 2.3. Experimental Method of Adaptability Evaluation

According to the adaptability of alkali and MDG, two experimental schemes were designed. Scheme 1: Considering the production source, the high-concentration MDG and high-concentration lye were mixed as the mother liquor, and the stability of the mother liquor at room temperature was observed. If the mother liquor can exist stably, the mother liquor is diluted with simulated water, which is beneficial to the transportation and preservation of the mother liquor. Scheme 2: From the perspective of wellhead injection, low-concentration MDG and low-concentration alkali are directly compounded to form a compound system and injected at the wellhead to investigate the adaptability of alkali and MDG. During the experiment, if the compound system in experimental Scheme 1 has poor adaptability, experimental Scheme 2 is adopted.

### 2.4. Experimental Methods of Basic Physical and Chemical Properties

Interfacial tension (IFT) was obtained by a TX-500C interfacial tensiometer (Kono Industrial Co., Ltd., Los Gatos, CA, UAS). The viscosity was obtained by a Brookfield DV-2 viscometer (Brookfield Viscometers Ltd., Harlow, UK) with a shear rate of 6 rpm at 50 °C. The wettability change ability of the MDG-strengthened-alkali-combination flooding system was obtained continuously by a JC2000D2 video optical contact angle measurement (POWEREACH, shanghai, China) at 50 °C. The emulsification performance was evaluated by the combination of evaluating the water absorption rate of the emulsion and observing the microscopic morphology of the emulsion by microscope.

### 2.5. Experimental Method of Crude-Oil-Production Mechanism

Through the single-tube core experimental model, the oil-displacement potential and crude-oil-production mechanism of the MDG-enhanced-alkali-compound systems were analyzed by using the online nuclear-magnetic-resonance experimental device. The experimental temperature was 50 °C. The simulated water and MDG-strengthened-alkali-compound system used in the experiment were all prepared with heavy water to shield the water-phase hydrogen signal. The experimental steps were as follows: the core (5 cm long, 2.5 cm in diameter) was weighed after drying, was vacuumized to saturate the simulated water, had the wet weight weighed, and had the pore volume calculated. Saturated oil was injected into the core at a rate of 0.1 mL/min, and the pump was stopped when

the liquid end did not produce water. After the core was aged for 24 h,  $T_2$ -spectrum scanning and imaging scanning were performed. The experiment was stopped when the water drive rate was 0.1 mL/min until the water cut of the output end was 98%. The injection pressure, water production, and oil production were recorded during the process, and  $T_2$ -spectrum scanning and imaging scanning were performed. The MDG-strengthened- $\text{Na}_2\text{CO}_3$ -compound system with a pore volume of 1 times was injected at a rate of 0.1 mL/min, and the experiment was stopped when the water content at the output end was 98%. The injection pressure, water production, and oil production were recorded during this process, and  $T_2$ -spectrum scanning and imaging scanning were performed. The MDG-strengthened- $\text{Na}_2\text{CO}_3$ -compound system was replaced by the MDG-strengthened- $\text{NaOH}$ -compound system, and the above steps were repeated. Figure 2 is the flow chart of online nuclear-magnetic-resonance displacement-experiment.

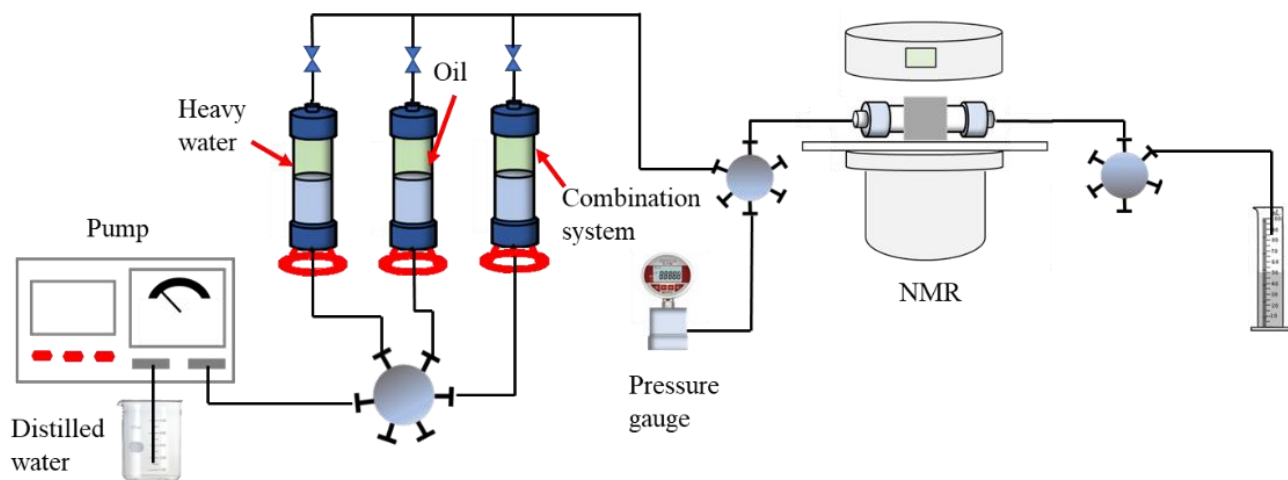


**Figure 2.** Online nuclear-magnetic-resonance displacement-experimental flow chart.

### 3. Results and Discussion

#### 3.1. Adaptability Evaluation

##### 3.1.1. Adaptability of Sodium Carbonate to MDG

The suitability of  $\text{Na}_2\text{CO}_3$  and MDG was investigated by experimental Scheme 1. When the concentration of  $\text{Na}_2\text{CO}_3$  was 15%, the compound system began to stratify after 3 days of aging, and the stratification was obvious after 5 days of aging. When the concentration of  $\text{Na}_2\text{CO}_3$  is 20%, the compound system is obviously stratified after aging for 3 days. When the concentration of  $\text{Na}_2\text{CO}_3$  is 10%, the compound system is still not layered after 60 days of aging, and the adaptability is good. According to Figure 3, when the concentration of  $\text{Na}_2\text{CO}_3$  is up to 10%, it has good compatibility with MDG. Therefore, 40% MDG and 10%  $\text{Na}_2\text{CO}_3$  are used as the compound system, and it can be stable for 60 days, which is in line with Scheme 1.

##### 3.1.2. The Suitability of Sodium Hydroxide and MDG

Scheme 1 was used to investigate the adaptability of high-concentration  $\text{NaOH}$  and high-concentration MDG. Under the condition of high-concentration  $\text{NaOH}$ , MDG showed obvious stratification and solution color change after 3 days of aging, and its stability was greatly affected by high-concentration  $\text{NaOH}$ . Therefore, Scheme 1 is not suitable for  $\text{NaOH}$ . Therefore, Scheme 2 was used to investigate the suitability of low-concentration  $\text{NaOH}$  and low-concentration MDG for further experiments. The experimental results are shown in Figures 4 and 5.

When the concentration of NaOH was 1.5%, MDG showed obvious stratification after 3 days of aging. When the concentration of NaOH was 1.0%, MDG only showed slight stratification after 60 days of aging, and the stability was good. It can be determined that NaOH was compounded with 1.0% and 5.0%.

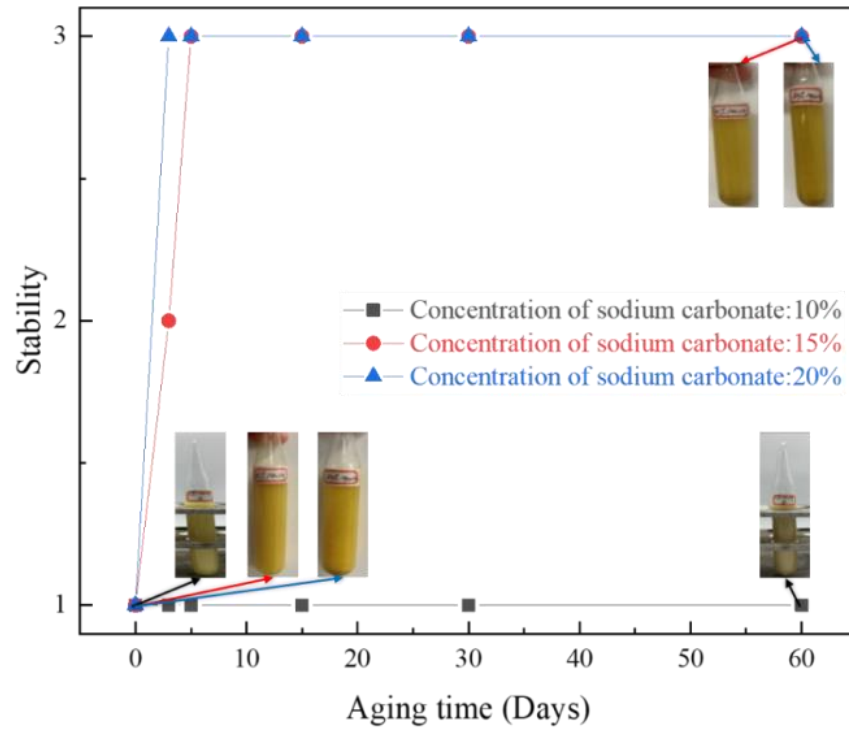


Figure 3. Compatibility of high-concentration sodium carbonate with MDG.

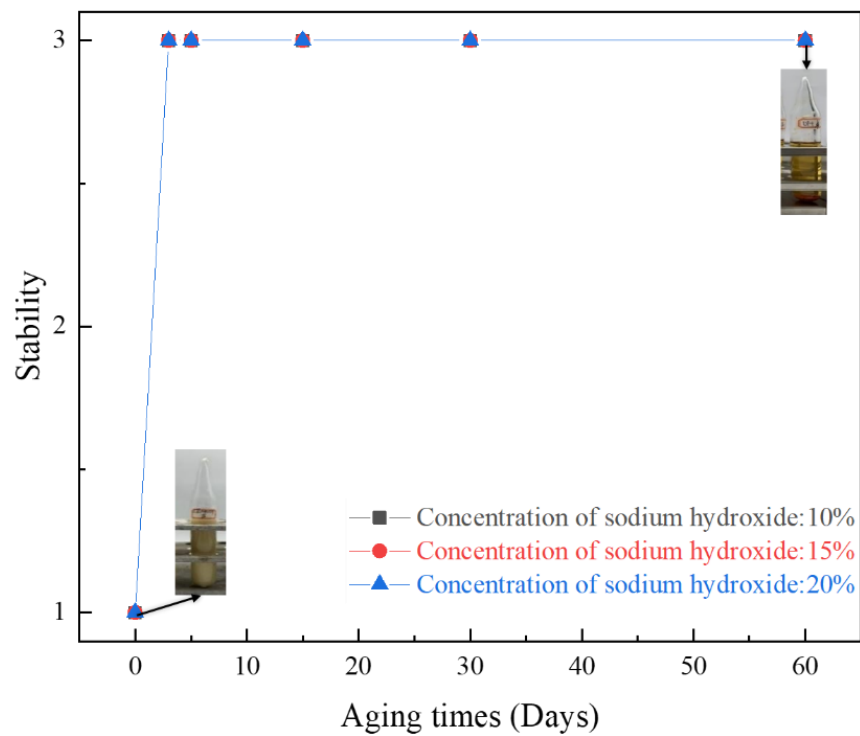
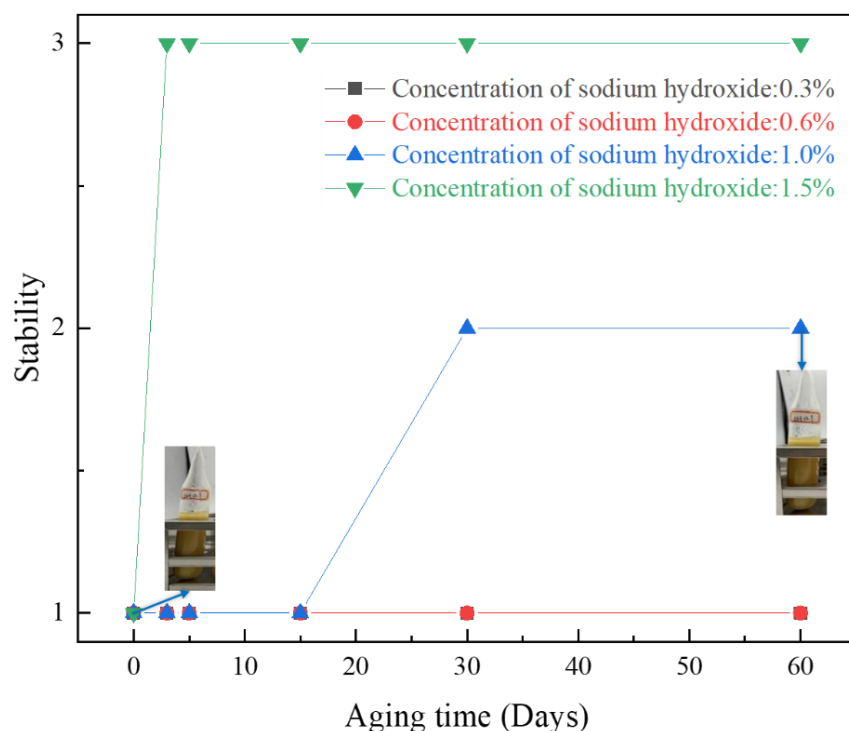


Figure 4. Compatibility of high-concentration sodium hydroxide with MDG.



**Figure 5.** Compatibility of low-concentration sodium hydroxide with MDG.

### 3.2. Physicochemical Properties

#### 3.2.1. Ability to Reduce Interfacial Tension

The lower the oil–water interfacial tension is, the more obvious the effect of enhanced oil recovery. Therefore, this section discusses the interfacial-tension characteristics of the compound system formed by the MDG-strengthened- $\text{Na}_2\text{CO}_3$  (MDGSC)-compound flooding system and MDG-strengthened- $\text{NaOH}$  (MDGSH)-compound flooding system.

#### Characteristics of Interfacial Tension of MDGSC-Compound Flooding System

In the previous section, it was determined that high-concentration MDG and high-concentration  $\text{Na}_2\text{CO}_3$  were mixed into mother liquor for the dilution of  $\text{Na}_2\text{CO}_3$ -complex MDG. Therefore, this section discussed the oil–water interfacial tension of the mother liquor and simulated water at different dilution ratios under different aging times. From Figure 6, with the increase in dilution ratio, the interfacial tension showed a trend of decreasing first and then increasing and reached the lowest value of  $10^{-2}$  mN/m when the dilution ratio was 1:4. When the dilution ratio is 1:9–1:1, the oil–water interfacial tension is low. Considering the cost, the dilution ratio is between 1:9–1:4. At this time, the compound system solves the problem of cost and low interfacial tension. At the same time, the interfacial tension of the compound system is higher than that of the single  $\text{Na}_2\text{CO}_3$  solution. This occurs because the MDG particles have a large surface area, and the surface will adsorb a part of the oil soap with interfacial activity, resulting in an increase in interfacial tension. From Figure 7, as the aging time increases, the oil–water interfacial tension of the compound system gradually decreases, which means that the interfacial tension of the compound system will be further reduced after the injection of the formation through the soaking process.

#### Characteristics of Interfacial Tension of MDGSH-Compound Flooding System

A total of 5.0% MDG was mixed with 0.3–1.5%  $\text{NaOH}$ , and the interfacial tension was compared with the ability of  $\text{NaOH}$  solution. The interfacial-tension changes of the compound system under different aging times were also investigated. From Figure 8, for the  $\text{NaOH}$  solution, the interfacial tension reaches the order of magnitude of  $10^{-1}$

mN/m when the mass concentration is 1.0%. When the concentration of NaOH is 1.5%, the oil–water interfacial tension reaches  $10^{-2}$  mN/m. However, because the concentration of NaOH is higher than 1.0%, it has a great influence on the stability of MDG. Therefore, combined with the adaptability of NaOH and MDG, when the concentration of NaOH is 1.0%, it can exert the best effect. At the same time, the interfacial tension of the compound system is significantly higher than that of the NaOH solution. This occurs because, due to the adsorption of the MDG particle interface, the rate of formation of interfacial active substances is slowed down and the interfacial active substances are also adsorbed to the surface of the MDG particles, resulting in a higher interfacial tension than the NaOH solution. It can be seen from Figure 9 that as the aging time increases, the oil–water–interfacial-tension value decreases slightly and then tends to be stable, which is also helpful for the interaction between the compound system and the crude oil during the oil recovery process.

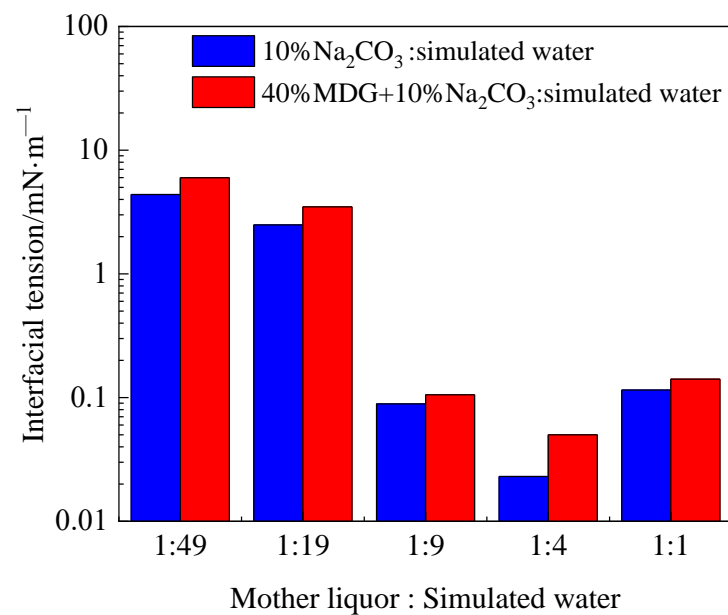


**Figure 6.** Effect of dilution ratio of MDGSC-compound system and simulated water on interfacial tension.

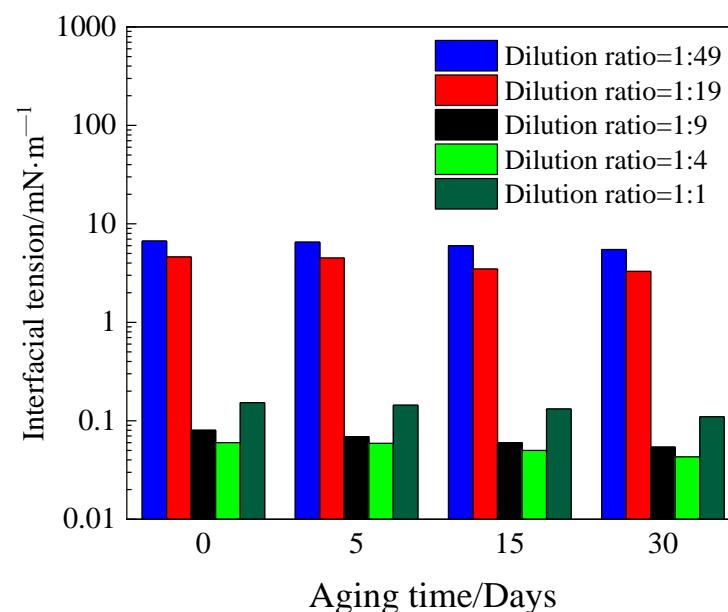


**Figure 7.** Effect of aging time on interfacial tension of MDGSC compound flooding system.

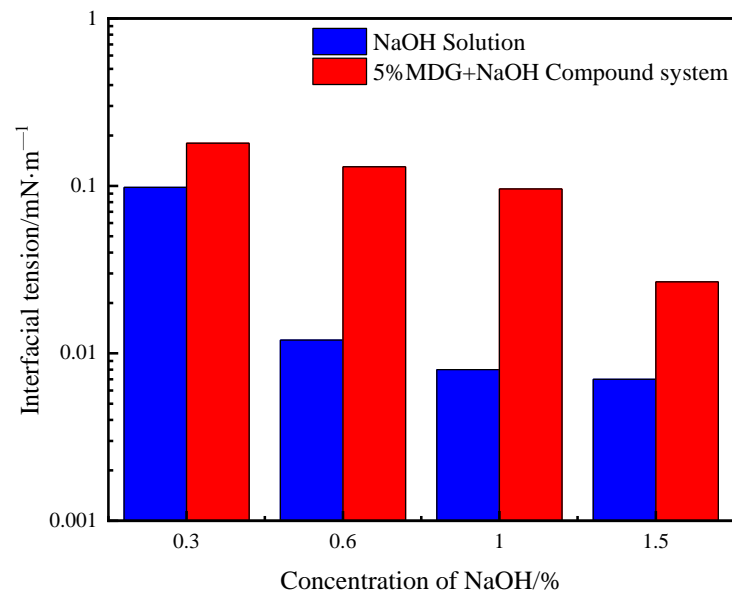


Figure 8. Effect of NaOH concentration on interfacial tension.

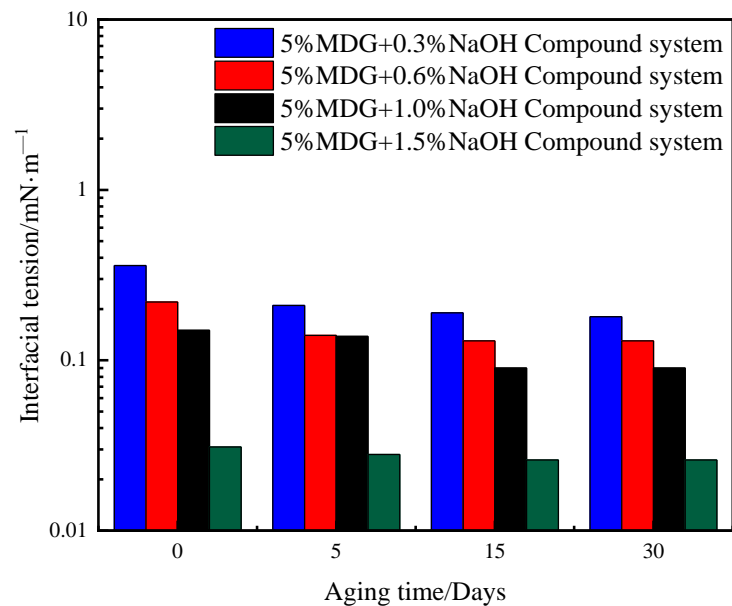


Figure 9. Effect of aging time on interfacial tension of MDGSH compound flooding system.

### 3.2.2. Viscosity Characteristics

Due to the large difference in water and oil viscosities, water flooding is prone to fingering. When the viscosity of the displacement fluid increases, the fingering problem can be alleviated. Therefore, the variation characteristics of viscosity of two MDG-strengthened-alkali-compound systems with aging time were investigated.

From Figure 10, the viscosity of the MDGSC-compound system is slightly lower than that of MDG alone. When the compound system is aged at  $50\text{ }^{\circ}\text{C}$  for 30 days, the viscosity retention rate is above 75%, and it still has good viscosity retention characteristics. From Figure 11, when the aging time increases, the viscosity of the MDGSH-compound system decreases. Compared with MDG, the viscosity of the MDGSH-compound system is greatly reduced. This occurs because NaOH compresses the diffusion electric double layer of the compound system particles, resulting in rapid coalescence between the compound system particles. The aggregates quickly coalesce and settle to the bottom of the container, and the solid content in the liquid phase of the compound system decreases, resulting in a greater decrease in the viscosity of the compound system than that of the individual MDG. After

30 days of aging, the viscosity retention rate of the compound system was greater than 72%. Although some particles of the compound system agglomerated, the viscosity retention of the compound system was higher after 30 days of aging, showing good storage stability.

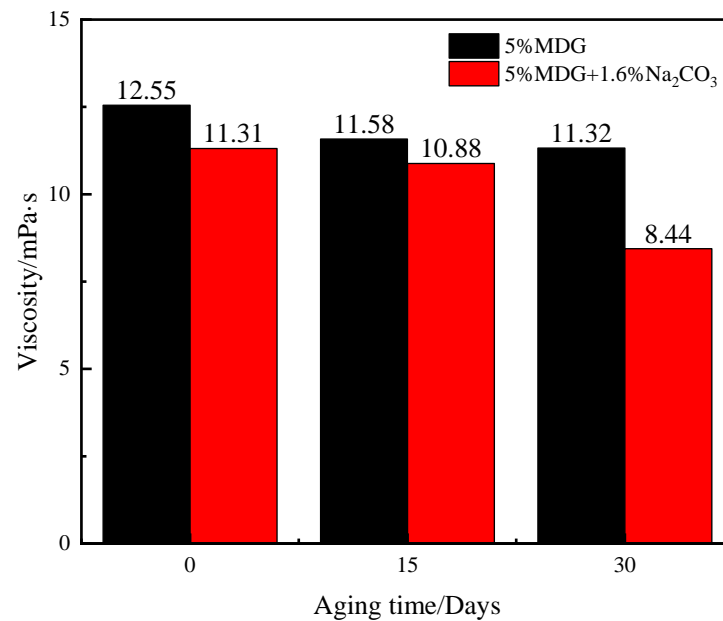


**Figure 10.** Effect of aging time on viscosity of MDGSC-compound system.

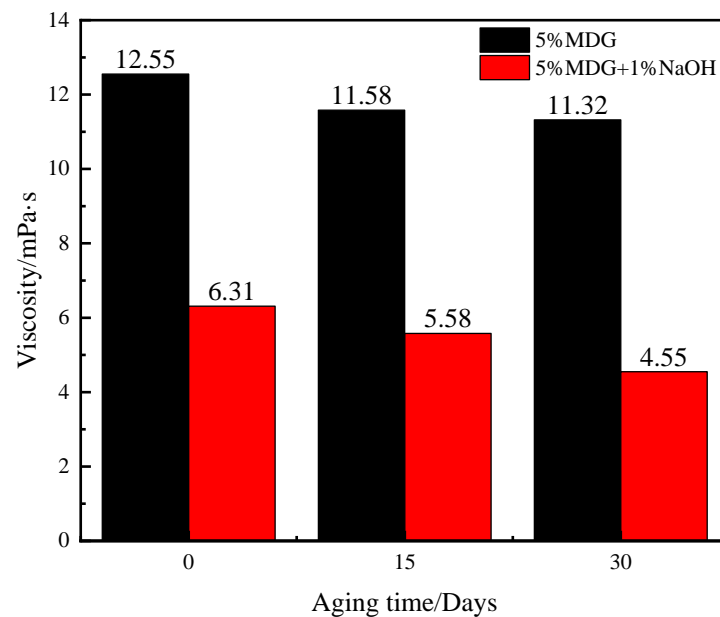


**Figure 11.** Effect of aging time on viscosity of MDGSH-compound system.

### 3.2.3. Emulsifying Ability

Emulsification is a phenomenon in which a liquid is uniformly dispersed in another immiscible liquid with very small droplets. The emulsion liquid phase is a thermodynamically unstable system due to its large interface area and high interface energy. In chemical flooding, after the interfacial active component contacts the underground crude oil, the crude oil will be emulsified to form smaller oil droplets that are evenly dispersed in the displacement fluid. Emulsification carrying and profile control of emulsion play an important role in enhancing oil recovery. Therefore, the water evolution rate and microstructure of MDG-strengthened-Na<sub>2</sub>CO<sub>3</sub>- and NaOH-compound emulsions at 50 °C were studied.

### Emulsifying Ability of MDGSC-Compound System

The water separation rate of the emulsion formed by the MDGSC-compound system and  $\text{Na}_2\text{CO}_3$  solution is shown in Figure 12. At the initial stage, the water separation rate increased rapidly, and the water separation rate gradually stabilized after 1.5 h of standing, and the stable value of the water separation rate of the emulsion formed by the  $\text{Na}_2\text{CO}_3$  solution was lower than that of the emulsion formed by the compound system. The water separation rate did not change after standing for 5 h, and the emulsion reached a stable state. When the initial state of the emulsion is formed, due to the high content of emulsion droplets, the oil soap molecules with interfacial activity are limited, and the oil soap molecules in the interfacial film are loosely arranged, so the strength of the formed interfacial film is low. At high temperature, the thermal motion of molecules in the interfacial film is intensified, the destruction process of the interfacial film is accelerated, the stability of the emulsion is deteriorated, and the water phase is precipitated rapidly. In the continuous aging, the precipitation of the aqueous phase leads to the decrease in the mass fraction of the emulsion droplets, the oil soap molecules form a directional adsorption arrangement on the interface film, the strength of the interface film increases, and the trend of the water separation rate of the emulsion slows down and stabilizes. The emulsion is uniformly dispersed in the initial state, and the interface energy is large. It is a thermodynamically unstable system. During the gradual aging, the oil droplets coalesce, the water phase is discharged, and the emulsion gradually reaches a stable state.

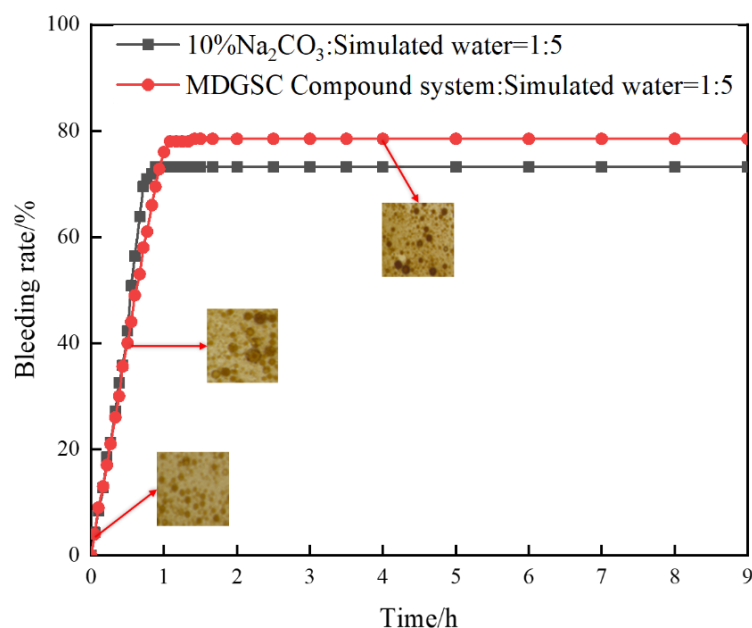


**Figure 12.** Stability of emulsion formed by MDGSC-compound system.

### Emulsifying Ability of MDGSH-Compound System

The water separation rate and stability of the emulsion formed by the 5.0% MDG and 1.0% NaOH compound system and 1.0% NaOH solution and crude oil were investigated. The experimental results are shown in Figure 13. From Figure 13, in the initial stage of the formation of the emulsion, the water separation rate of the system increased rapidly and gradually stabilized after standing for 0.5 h, and the water separation rate of the emulsion remained basically unchanged after standing for 2 h. Because the oil–water–interfacial-tension value of the reinforced-NaOH-compound system is lower than that of the other two systems, the stable value of the water separation rate after the formation of the emulsion is also the lowest, and the emulsion is relatively stable. Although the oil–water–interfacial-tension value of the MDG-strengthened-NaOH-compound system can reach the ultra-low interfacial-tension level, due to the high mass fraction of droplets in the initial state after the formation of emulsion, the limited number of interfacial active molecules also leads to

the low strength of the interfacial film, and the water phase continues to precipitate from the droplets. The emulsion droplets gradually agglomerated from the uniform dispersion state, and the emulsion gradually reached a stable state.

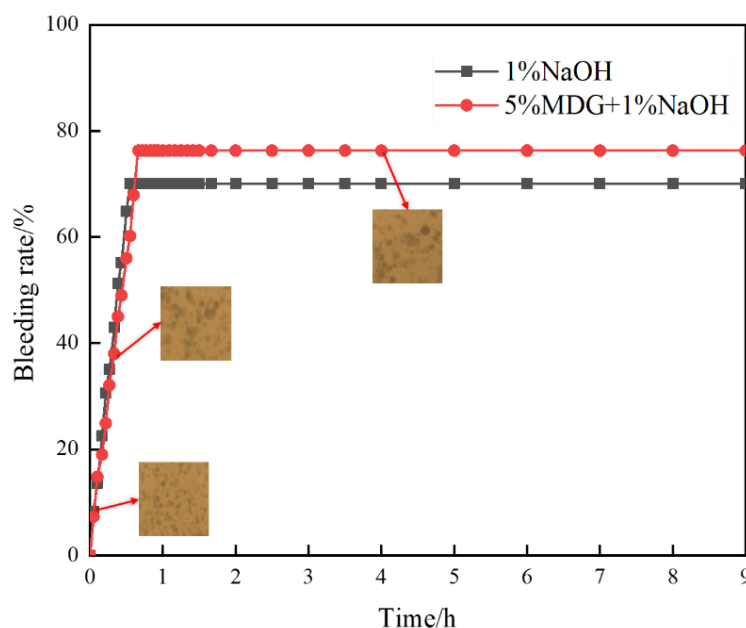


**Figure 13.** Stability of emulsion formed by MDGSH-compound system.

### 3.2.4. Wetting Change Ability

The wettability of the formation rock has a great influence on the oil-film-stripping effect of the displacement fluid. If the formation sandstone is reversed from oil-wet to water-wet surface after the action of the displacement fluid, the oil film attached to the sandstone will be easily stripped to improve oil recovery. The wetting ability of MDG-strengthened- $\text{Na}_2\text{CO}_3$ - and NaOH-compound systems at 50 °C was investigated.

#### Wetting Change Ability of MDGSC-Compound System

The wetting ability of the MDGSC-compound system on oil-wet quartz flakes at 50 °C was investigated. From Figure 14, for oil-wet quartz flakes, in the process of continuous aging, the oil-phase wetting angle of the compound system gradually changes from 23.9° of the initial state to 140.1°. The oil-wet quartz flakes are reversed from the oil-wet surface to the water-wet surface, which helps to better strip the oil film attached to the sandstone surface. At the same time, the wetting reversal ability of  $\text{Na}_2\text{CO}_3$  solution alone is stronger, which is similar to the law of oil–water interfacial tension. The oil soap with interfacial activity generated by the reaction of  $\text{Na}_2\text{CO}_3$  and petroleum acid is more adsorbed to the oil–water interface, the oil–water interfacial tension is lower, and the wetting change ability is stronger. This property of the MDGSC-compound system can effectively strip the crude oil attached to the rock surface.

#### Wetting Change Ability of MDGSH-Compound System

The wetting ability of MDGSH-compound system on oil-wet quartz sheets at 50 °C was investigated. The experimental results are shown in Figure 15. From Figure 15, the NaOH solution and MDGSH-compound system increase the wetting angle of the oil phase, the wettability of the oil-wet quartz plate is reversed to water wettability, and the time to achieve wetting reversal is the shortest. After 15 days of aging, the wettability of the quartz plate in the MDGSH-compound system is completely reversed to water wettability. The surface-active substance generated by the reaction of NaOH and petroleum acid realizes the effect of adsorption and desorption on the quartz plate to achieve a dynamic balance.

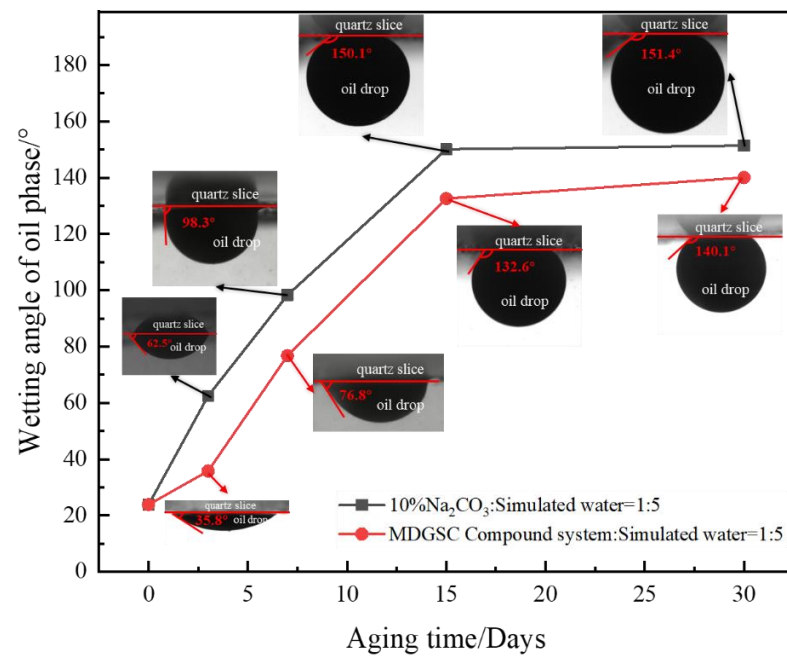


Figure 14. Wetting change ability of MDGSC-compound system.

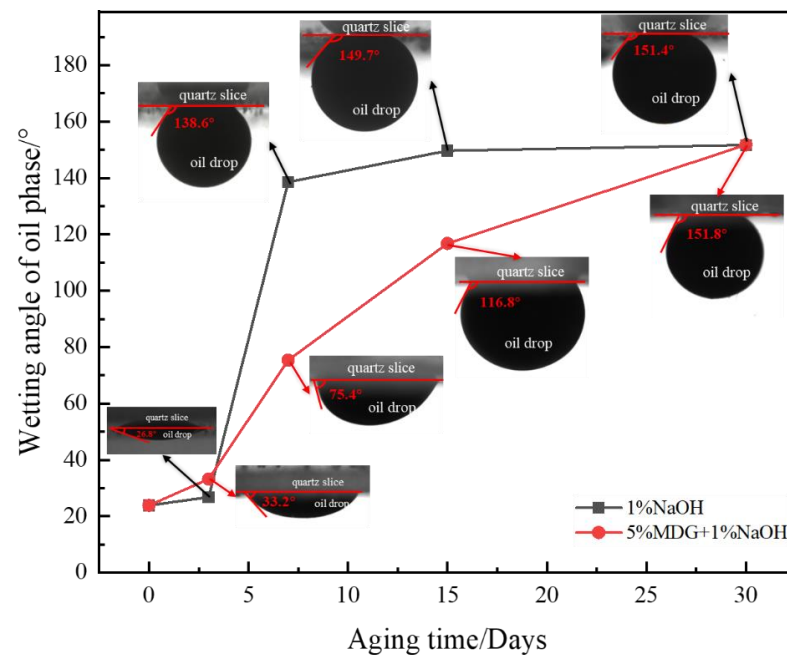


Figure 15. Wetting change ability of MDGSH-compound system.

### 3.3. Crude-Oil-Production Mechanism

The enhanced-oil-recovery ability and crude-oil-production mechanism of the two compound systems of MDGSC and MDGSH in compound flooding systems for low permeability cores were studied.

Figures 16 and 17 show the oil-displacement capacity of two compound systems of MDGSC and MDGSH through a single-tube core flooding experimental model. It can be seen from Figures 16 and 17 that after the two compound systems of 1PV are injected, respectively, the enhanced oil recovery of the MDGSC-compound system is 40.31%, and the enhanced oil recovery of the MDGSH-compound system is 43.22%. When the water cut of the produced fluid exceeds 98%, the enhanced oil recovery of the MDGSC-compound system is 43.91%, and the enhanced oil recovery of the MDGSH-compound system is

47.78%. Both of them show good enhanced-oil-recovery ability at different displacement stages, but there are also differences. This occurs because MDG can directly block pore throats smaller than a single particle size, and through the aggregation and expansion between particles and mutual bridging, the high permeability macropores in the core are blocked, forcing the subsequent injection water to flow and expand the sweep. The MDGSH-compound system has better ability to improve oil recovery. This occurs because it is easier to achieve ultra-low interfacial tension with crude oil. At the same time, it interacts with the rock surface and crude oil so that the surface of the oil-wet rock is transformed into a hydrophilic rock surface. The ability to change the wettability of the rock surface is stronger than that of the MDGSC-compound system. The remaining oil in the water-channeling channel and more remaining oil in the unswept area are displaced to achieve efficient stripping of the remaining oil on the rock surface. Although the enhanced oil recovery of the MDGSC-compound system is weaker than that of the MDGSH-compound system, it still shows good oil-displacement effect.

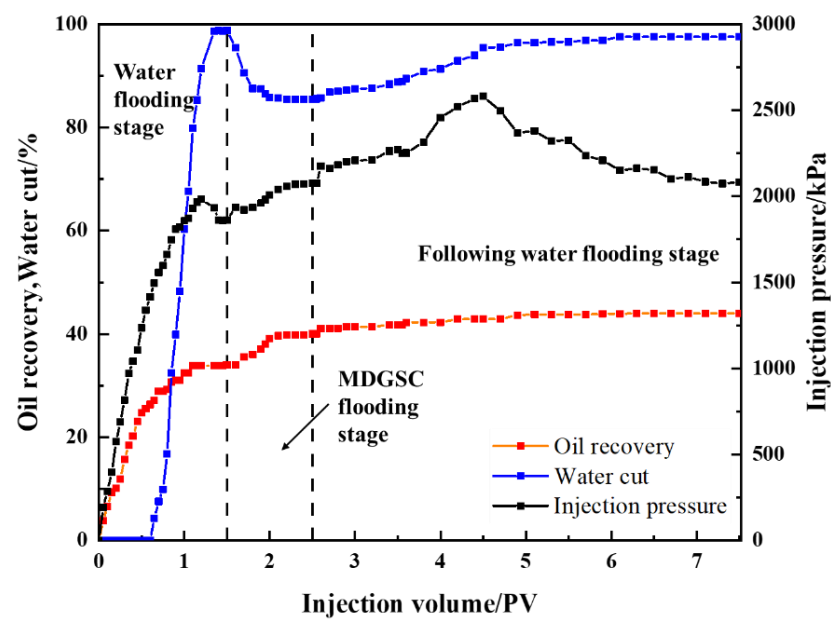


Figure 16. Enhanced-oil-recovery capacity of MDGSC-compound flooding system.

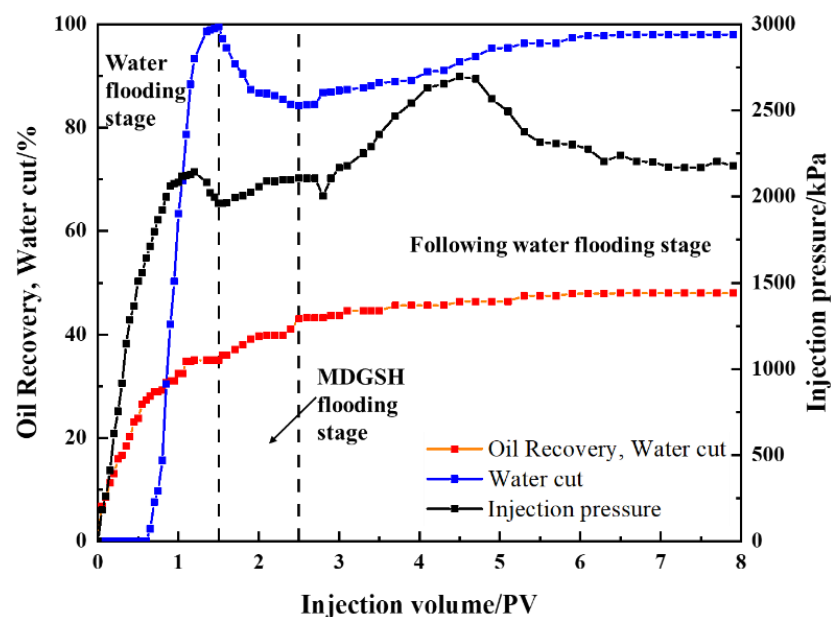
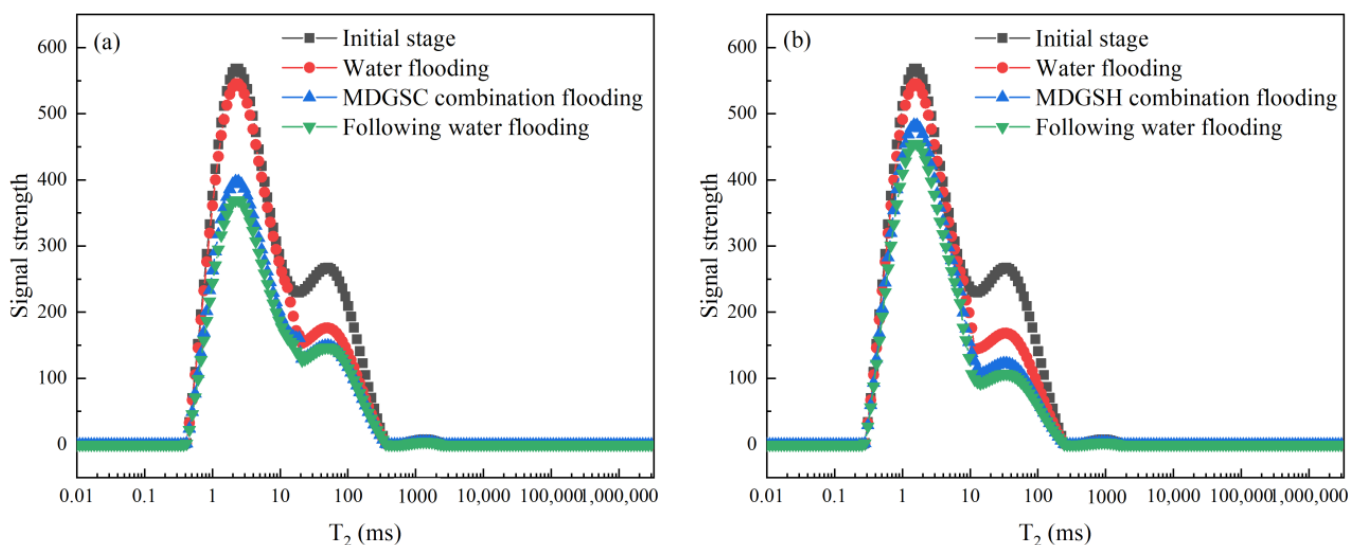
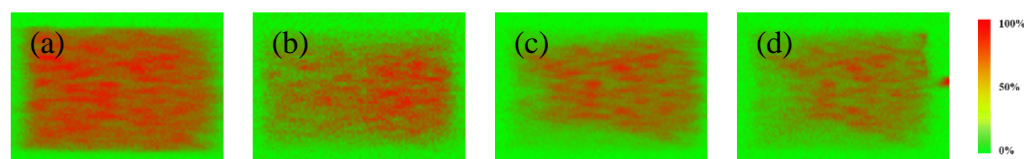


Figure 17. Enhanced-oil-recovery capacity of MDGSH-compound flooding system.

At the same time, the online nuclear-magnetic-resonance displacement-experimental device is used to further illustrate the crude-oil-production mechanism of the two compound systems. Figures 18–20 are the  $T_2$ -spectrum curves and remaining-oil distribution of the two compound systems at different displacement stages. From Figure 18, the characteristic peaks of the  $T_2$  curve are mainly concentrated in 0.1–10 ms, that is, the crude oil is mainly stored in small pores, and there are also signal quantities with characteristic peaks greater than 10 ms. This is due to the development of large-sized micro-fractures in the core, and some crude oil is also distributed here. The main distribution of crude oil in the core imaging results is also basically consistent with the  $T_2$  curve. For the displacement process of the two compound systems, after water flooding, the semaphore with a characteristic peak of 10–100 ms decreased, while the semaphore with a characteristic peak of 0.1–10 ms remained basically unchanged. From the  $T_2$  curve, the recovery of large pores in the MDGSC-compound system is 42.9%, and the recovery of small pores is 35.1%. The recovery of large pores in the MDGSH-compound system is 56.9%, and the recovery of small pores is 20.1%. When the 1PV-compound flooding system is injected and has subsequent water flooding, the signal quantity in the large pores and small pores of the two compound systems decreases. The decrease in the small pore signal quantity of the MDGSC-compound system is higher than that of the MDGSH-compound system. The oil recovery rates of small pores are 31.1% and 16.2%, while the signal quantity in the large pores of the MDGSH-compound system decreases greatly, and the recovery rate is 22.5%, which is higher by 7.4% than that of the MDGSC-compound system. This means that the MDGSC-compound system is more effective in plugging micro-fractures and continuously expanding the remaining oil in the small pores, while the MDGSH-compound system has a relatively weak performance in plugging micro-fractures, but its high-efficiency oil-washing ability can wash out most of the remaining oil in micro-fractures, and it also has the ability to expand the spread volume; combined with the analysis of the physical and chemical properties of the two compound systems, the MDGSC-compound system has a relatively weak ability to reduce the interfacial tension and wetting reversal ability, but its stability is strong, and it can form an effective plugging in the micro-fractures and continue to expand the spread volume. The stability of the MDGSH-compound system is weak, and a certain degree of plugging is formed on the micro-fractures, but its ability to reduce the interfacial tension and wetting change ability is excellent, and the remaining oil in the micro-fractures is efficiently washed out. The two mechanisms for crude oil production are different, but each has its own characteristics.



**Figure 18.** The changes of signal strength for  $T_2$  in the injection of different compound flooding systems. (a)  $T_2$  curve of MDGSC-compound flooding system. (b)  $T_2$  curve of MDGSH-compound flooding system.



**Figure 19.** The changes of oil saturation in the injection of MDGSC-compound flooding system. (a) Initial stage. (b) Water flooding. (c) MDGSC-compound flooding. (d) Following water flooding.

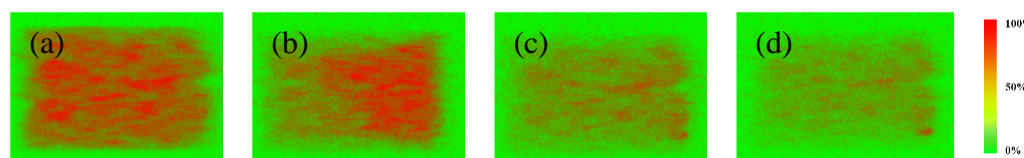


**Figure 20.** The changes of oil saturation in the injection of MDGSH-compound flooding system. (a) Initial stage. (b) Water flooding. (c) MDGSC-compound flooding. (d) Following water flooding.

#### 4. Conclusions

In this paper, a new type of microgel (MDG)-enhanced-alkali-compound flooding system was proposed for high-water-cut and heterogeneity oilfields. The compatibility of sodium carbonate, sodium hydroxide, and MDG was investigated. The basic physical and chemical properties of the compound system were evaluated, and its enhanced-oil-recovery ability and crude-oil-production mechanism were studied. The high concentration of MDG (40%) and high concentration of sodium carbonate (10%) have good adaptability, and the configuration as mother liquor is conducive to preservation and transportation. The mother liquor and the injected water can be directly mixed and injected according to the dilution ratio of 1:5 when it is used in a wellhead. At the same time, the MDGSC-compound system can reduce the interfacial tension up to  $10^{-2}$  mN/m. The interfacial tension decreases with the increase in aging time, and its viscosity also has a good viscosity retention rate with the aging time. The stability of the emulsion is moderate, and the wetting reversal can be achieved within 10 days, which effectively strips the crude oil from the rock wall. The adaptability of high-concentration MDG and high-concentration NaOH is poor, and the compound system appears to have obvious stratification in a short time. Therefore, the MDGSH-compound system is formed by mixing low-concentration MDG and low-concentration NaOH. The interfacial tension of the system is reduced to  $10^{-2}$  mN/m level, and the viscosity retention rate is still 72% after 30 days of aging. The emulsion is relatively stable, and the wettability reversal of rock wall can be realized within 7 days.

The enhanced oil recovery of the MDGSC-compound flooding system is 43.91%, and the enhanced oil recovery of the MDGSH-compound flooding system is 47.78%. The MDGSC-compound flooding system is more effective in plugging micro-fractures and continuously expanding the swept volume, while the MDGSH-compound flooding system has relatively weak performance in plugging micro-fractures, but its oil-washing ability can flush out the remaining oil in micro-fractures. The MDGSC-compound flooding system has a relatively weak ability to reduce interfacial tension and wettability reversal, but its stability is strong, and it can form effective plugging in micro-fractures to continuously expand and spread. The stability of the MDGSH-compound flooding system is weak, and it plugs the micro-fractures. Its ability to reduce interfacial tension and wetting change is excellent, and the remaining oil in the micro-fractures is efficiently washed out. The crude-oil-production mechanism of the two compound flooding systems is clarified.

**Author Contributions:** T.W. (Teng Wang): Conceptualization, Methodology, Investigation, Formal analysis, and Writing—original draft. T.W. (Tianjiang Wu): Investigation, Methodology, Conceptualization, and Supervision. Y.L.: Investigation, Formal analysis, and Methodology. C.C.: Conceptualization, Methodology, and Writing—original draft. G.Z.: Conceptualization and Supervision. All authors have read and agreed to the published version of the manuscript.

**Funding:** This research received no external funding.

**Data Availability Statement:** Data available on request due to restrictions. The data presented in this study are available on request from the corresponding author due to the privacy.

**Acknowledgments:** The authors express their gratitude to the authors of the references cited in this article, as well as to the School of Petroleum Engineering at China University of Petroleum (East China) and the Oil and Gas Technology Research Institute of Changqing Oilfield for their support and assistance in the research conducted in this article. The authors also express their sincere gratitude to the reviewers for their efforts and the suggested revisions.

**Conflicts of Interest:** Author Teng Wang, Tianjiang Wu, Yunlong Liu, Chen Cheng were employed by the company PetroChina Changqing Oilfield Company. The remaining author declare that the research was conducted in the absence of any commercial or financial relationships that could be construed as a potential conflict of interest. The company had no role in the design of the study; in the collection, analyses, or interpretation of data; in the writing of the manuscript, or in the decision to publish the results.

## References

1. Ming, Y. The optimization of the well pattern thinning at high water cut stages in CD Heterogeneity oilfield. *Unconv. Resour.* **2024**, *4*, 100063. [[CrossRef](#)]
2. He, M.; Pu, W.; Yang, X.; Liu, R.; Xu, M.; Li, X.; Wu, T.; Gou, R. Experimental study on the effect of high water cut on the emulsifying properties of crude oil. *Colloids Surf. A Physicochem. Eng. Asp.* **2023**, *674*, 131917. [[CrossRef](#)]
3. Yu, H.; Wang, Y.; Zhang, L.; Zhang, Q.; Guo, Z.; Wang, B.; Sun, T. Remaining oil distribution characteristics in an oil reservoir with ultra-high water-cut. *Energy Geosci.* **2022**, *5*, 100116. [[CrossRef](#)]
4. Guo, H.; Cheng, L.; Jia, P. Quantitative investigation of core heterogeneity's impact on water flooding using nuclear magnetic resonance imaging. *Chem. Eng. Sci.* **2023**, *282*, 119186. [[CrossRef](#)]
5. Zhao, W.; Zhao, L.; Jia, P.; Wang, P.; Hou, J. Influence of micro-heterogeneity of fractured-porous reservoirs on the water flooding mobilization law. *Sustain. Energy Technol. Assess.* **2022**, *53*, 102694. [[CrossRef](#)]
6. Wei, J.; Zhang, D.; Zhang, X.; Zhao, X.; Zhou, R. Experimental study on water flooding mechanism in low permeability oil reservoirs based on nuclear magnetic resonance technology. *Energy* **2023**, *278*, 127960. [[CrossRef](#)]
7. Wei, J.; Zhou, X.; Zhou, J.; Li, J.; Wang, A. Recovery efficiency of tight oil reservoirs with different injection fluids: An experimental investigation of oil-water distribution feature. *J. Pet. Sci. Eng.* **2020**, *195*, 107678. [[CrossRef](#)]
8. Lei, X.; Zhao, C.; Zhang, Q.; Wang, P.; Xiong, R. Effect of high-multiple water injection on rock pore structure and oil displacement efficiency. *Energy Geosci.* **2022**, *5*, 100137. [[CrossRef](#)]
9. Li, Q.; Liu, J.; Wang, S.; Guo, Y.; Han, X.; Li, Q.; Cheng, Y.; Dong, Z.; Li, X.; Zhang, X. Numerical insights into factors affecting collapse behavior of horizontal wellbore in clayey silt hydrate-bearing sediments and the accompanying control strategy. *Ocean. Eng.* **2024**, *297*, 117029. [[CrossRef](#)]
10. Li, Q.; Wang, Y.; Owusu, A.B. A modified Ester-branched thickener for rheology and wettability during CO<sub>2</sub> fracturing for improved fracturing property. *Environ. Sci. Pollut. Res.* **2019**, *26*, 20787–20797. [[CrossRef](#)]
11. Kamari, A.; Sattari, M.; Mohammadi, A.H.; Ramjugernath, D. Reliable method for the determination of surfactant retention in porous media during chemical flooding oil recovery. *Fuel* **2015**, *158*, 122–128. [[CrossRef](#)]
12. Bhatkar, S.A.; Bhadane, N.P.; Kshirsagar, L.K.; Wadgaonkar, V.S. Modifications of petroleum industry effluent treatment Method: An approach for quality improvement of process water for ASP flooding and chemical EOR. *Mater. Today Proc.* **2023**, *77*, 371–375. [[CrossRef](#)]
13. Guo, Y.-B.; Yue, X.-A.; Yang, C.-C. New method to quantitatively characterize the emulsification capability of chemical flooding agents. *J. Pet. Sci. Eng.* **2021**, *196*, 107810. [[CrossRef](#)]
14. Cao, H.; Li, Y.; Gao, W.; Cao, J.; Sun, B.; Zhang, J. Experimental investigation on the effect of interfacial properties of chemical flooding for enhanced heavy oil recovery. *Colloids Surf. A Physicochem. Eng. Asp.* **2023**, *677*, 132335. [[CrossRef](#)]
15. Pang, S.; Pu, W.; Jiang, F.; Gao, H.; Wang, Y.; Chen, Y.; Wei, P. Effect of water content on features of W/O emulsion during water flooding in heavy oil reservoir: Bulk properties and mobility control characteristics. *J. Pet. Sci. Eng.* **2021**, *207*, 109075. [[CrossRef](#)]
16. Tian, W.; Lu, S.; Zhang, J.; Gao, Y.; Huang, W.; Wen, Z.; Li, J.; Li, J. NMR characterization of fluid mobility in low-permeability conglomerates: An experimental investigation of spontaneous imbibition and flooding. *J. Pet. Sci. Eng.* **2022**, *214*, 110483. [[CrossRef](#)]
17. Nowrouzi, I.; Mohammadi, A.H.; Manshad, A.K. Water-oil interfacial tension (IFT) reduction and wettability alteration in surfactant flooding process using extracted saponin from *Anabasis Setifera* plant. *J. Pet. Sci. Eng.* **2020**, *189*, 106901. [[CrossRef](#)]
18. Liu, X.; Chen, Z.; Cui, Z. Foaming systems for foam flooding with both high foaming performance and ultralow oil/water interfacial tension. *J. Mol. Liq.* **2022**, *355*, 118920. [[CrossRef](#)]
19. Wang, Y.; Liu, H.; Zhang, Q.; Chen, Z.; Wang, J.; Dong, X.; Chen, F. Pore-scale experimental study on EOR mechanisms of combining thermal and chemical flooding in heavy oil reservoirs. *J. Pet. Sci. Eng.* **2020**, *185*, 106649. [[CrossRef](#)]

20. Wu, D.; Zhou, K.; Hou, J.; An, Z.; Zhai, M.; Liu, W. Experimental study on combining heterogeneous phase composite flooding and streamline adjustment to improve oil recovery in heterogeneous reservoirs. *J. Pet. Sci. Eng.* **2020**, *194*, 107478. [[CrossRef](#)]
21. Wang, L.; Li, S.; Cao, R.; Han, P.; Yan, W.; Sun, G.; Xia, H.; Xu, T. Microscopic plugging adjustment mechanism in a novel heterogeneous combined flooding system. *Energy Rep.* **2022**, *8*, 15350–15364. [[CrossRef](#)]
22. Wang, Y.; Zhang, J.; Yang, S.-L.; Xu, Z.-X.; Cheng, S.-Q. Pressure transient characteristics of non-uniform conductivity fractured wells in viscoelasticity polymer flooding based on oil–water two-phase flow. *Pet. Sci.* **2023**, *21*, 343–351. [[CrossRef](#)]
23. Seright, R.; Wang, D. Polymer flooding: Current status and future directions. *Pet. Sci.* **2023**, *20*, 910–921. [[CrossRef](#)]
24. Li, X.; Yan, Z.; Wei, K.; Zhu, X.; Zhu, L.; Huo, T.; Li, Y.; Xue, Q. Pore-scale investigation on the flow behavior and oil displacement of ultralow IFT surfactant flooding based on CFD simulation. *Colloids Surf. A Physicochem. Eng. Asp.* **2023**, *679*, 132555. [[CrossRef](#)]
25. An, Z.-B.; Zhou, K.; Wu, D.-J.; Hou, J. Production characteristics and displacement mechanisms of infilling polymer-surfactant-preformed particle gel flooding in post-polymer flooding reservoirs: A review of practice in Ng3 block of Gudao Oilfield. *Pet. Sci.* **2023**, *20*, 2354–2371. [[CrossRef](#)]
26. Li, Y.-B.; Jia, H.-F.; Pu, W.-F.; Wei, B.; Wang, S.-S.; Yuan, N. Investigation of feasibility of alkali–cosolvent flooding in heavy oil reservoirs. *Pet. Sci.* **2023**, *20*, 1608–1619. [[CrossRef](#)]
27. Wang, T.; Xuan, Y.; Lv, D.; Xie, Z.; Zhao, G.; Dai, C. Potential application of dispersed particle gel strengthened alkali as a novel combination flooding system for enhanced oil recovery. *J. Mol. Liq.* **2022**, *368*, 120816. [[CrossRef](#)]
28. Gong, Y.; Li, L.; Huang, W.; Zou, J.; Zhong, X.; Wang, L.; Kang, D.; Zhang, Z.; Zhang, Z. A study of alkali-silica nanoparticle-polymer (ANP) flooding for enhancing heavy oil recovery. *J. Pet. Sci. Eng.* **2022**, *213*, 110465. [[CrossRef](#)]
29. Sharma, H.; Panthi, K.; Mohanty, K.K. Surfactant-less alkali-cosolvent-polymer floods for an acidic crude oil. *Fuel* **2018**, *215*, 484–491. [[CrossRef](#)]
30. Ahmed, S.; Hanamertani, A.S.; Alameri, W.; Al-Shalabi, E.W.; Hashmet, M.R. Experimental investigation of flow diversion and dynamic retention during polymer flooding in high salinity fractured carbonates using CT imaging. *Geoenergy Sci. Eng.* **2023**, *221*, 211349. [[CrossRef](#)]
31. Zhu, W.; Li, H.; Chen, Z.; Song, Z. Pore-scale experiments reveal distinct flow field of polymer flooding with viscoelasticity loss by high salinity. *Colloids Surf. A Physicochem. Eng. Asp.* **2023**, *668*, 131473. [[CrossRef](#)]
32. Zhu, D.-Y.; Luo, R.-T.; Liu, Y.; Qin, J.-H.; Zhao, Q.; Zhang, H.-J.; Wang, W.-S.; Wang, Z.-Y.; Zhu, M.-E.; Wang, Y.-P.; et al. Development of re-crosslinkable dispersed particle gels for conformance improvement in extremely high-temperature reservoirs. *Pet. Sci.* **2022**, *19*, 2922–2931. [[CrossRef](#)]
33. Zhu, Z.X.; Li, L.; Liu, J.W.; Chen, J.; Xu, Z.Z.; Wu, Y.N.; Dai, C.L. Probing the effect of Young’s modulus on the plugging performance of micro-nano-scale dispersed particle gels. *Pet. Sci.* **2022**, *19*, 688–696. [[CrossRef](#)]
34. Yang, N.; Ma, H.; Bo, Q.; Li, J.; Sun, N.; Dai, C.; Zhao, G. A novel fluorescent dispersed particle gel: Fluorescence monitoring method and breakthrough flow channel identification. *J. Mol. Liq.* **2023**, *385*, 122219. [[CrossRef](#)]
35. Sun, N.; Yao, X.; Liu, J.; Li, J.; Yang, N.; Zhao, G.; Dai, C. Breakup and coalescence mechanism of high-stability bubbles reinforced by dispersed particle gel particles in the pore-throat micromodel. *Geoenergy Sci. Eng.* **2023**, *223*, 211513. [[CrossRef](#)]
36. Wang, W.; Guo, X.; Duan, P.; Kang, B.; Zheng, D.; Zafar, A. Investigation of plugging performance and enhanced oil recovery of multi-scale polymer microspheres in low-permeability reservoirs. *Nat. Gas Ind. B* **2023**, *10*, 223–232. [[CrossRef](#)]
37. Li, Y.-K.; Hou, J.-R.; Wu, W.-P.; Qu, M.; Liang, T.; Zhong, W.-X.; Wen, Y.-C.; Sun, H.-T.; Pan, Y.-N. A novel profile modification HPF-Co gel satisfied with fractured low permeability reservoirs in high temperature and high salinity. *Pet. Sci.* **2023**, *21*, 683–693. [[CrossRef](#)]
38. Li, B.; Zou, C.; Liang, H.; Chen, W.; Lin, S.; Liao, Y. Mass transfer from nanofluid single drops in low interfacial tension liquid–liquid extraction process. *Chem. Phys. Lett.* **2021**, *771*, 138530. [[CrossRef](#)]
39. Jia, R.; Kang, W.; Li, Z.; Yang, H.; Gao, Z.; Zheng, Z.; Yang, H.; Zhou, B.; Jiang, H.; Turtabayev, S. Ultra-low interfacial tension (IFT) zwitterionic surfactant for imbibition enhanced oil recovery (IEOR) in tight reservoirs. *J. Mol. Liq.* **2022**, *368*, 120734. [[CrossRef](#)]
40. Liu, J.; Liu, S.; Zhong, L.; Wang, P.; Gao, P.; Guo, Q. Ultra-low interfacial tension Anionic/Cationic surfactants system with excellent emulsification ability for enhanced oil recovery. *J. Mol. Liq.* **2023**, *382*, 121989. [[CrossRef](#)]
41. Feng, S.; Jiang, Z.; Tang, S.; Hu, R.; Jin, L.; Wang, S.; Wang, R. Synthesis, interfacial activity and rheological properties of low interfacial tension viscoelastic Gemini surfactants. *J. Pet. Sci. Eng.* **2022**, *209*, 109845. [[CrossRef](#)]
42. Tetteh, J.; Bai, S.; Kubelka, J.; Piri, M. Wettability reversal on oil-wet calcite surfaces: Experimental and computational investigations of the effect of the hydrophobic chain length of cationic surfactants. *J. Colloid Interface Sci.* **2022**, *619*, 168–178. [[CrossRef](#)] [[PubMed](#)]
43. Tetteh, J.; Kubelka, J.; Piri, M. Effect of oil carboxylate hydrophobicity on calcite wettability and its reversal by cationic surfactants: An experimental and molecular dynamics simulation investigation. *J. Mol. Liq.* **2023**, *380*, 121663. [[CrossRef](#)]

**Disclaimer/Publisher’s Note:** The statements, opinions and data contained in all publications are solely those of the individual author(s) and contributor(s) and not of MDPI and/or the editor(s). MDPI and/or the editor(s) disclaim responsibility for any injury to people or property resulting from any ideas, methods, instructions or products referred to in the content.